Experimental Study of Heat and Mass Transfer During Steam Injection in Homogeneous Porous Media

S. Peralta, A. Torres, F. Aragón, G. Domínguez Zacarías, A. Medina and A. López-Villa

Abstract We carry out experiments in which we have already measured, in a short period of time, the physical parameters that appear during the steam injection in a homogenous porous media (Woods and Fitzgerald 1993). For this work, we measured the distribution of displacement and temperature that occurred when steam is injected at different pressures (0.25–1 kg/cm^2) in a homogeneous porous media by the control of the injection pressure and flow rate.

1 Introduction

The displacement of a fluid through a porous medium has been a topic of interest because of its relevance in the recovery of oil (Chung and Butler 1989b). Most thermal recovery methods have been applied to high viscosity oil reservoirs with the objective of increasing oil production by reducing oil viscosity. Heat can be injected into the reservoir as hot water or steam, or can be generated in-situ by burning part of

S. Peralta (✉) · A. Torres
Instituto Mexicano del Petróleo, Eje Central Lázaro Cárdenas 152, Col. Atepehuacán, Distrito Federal, 07730 México, DF, México
e-mail: peraltasalomon@hotmail.com

F. Aragón
SEPI-ESIME Zacatenco, Av. Instituto Politécnico Nacional s/n, Unidad Profesional "Adolfo López Mateos", Col. Lindavista, Del. Gustavo A. Madero, C.P. 07738 México, DF, México

G. D. Zacarías
Cordinación Tecnológica de Ingeniería de Yacimientos, Eje Central Lázaro Cárdenas Norte 152 Col. San Bartolo Atepehuacán, Del. Gustavo A. Madero, C.P. 07730 México, DF, México

A. Medina and A. López-Villa
SEPI-ESIME-Azcapotzalco. Instituto Politécnico Nacional, Av. de las Granjas 682, Col. Santa Catarina, Azcapotzalco, 02250 México, DF, México

J. Klapp and A. Medina (eds.), *Experimental and Computational Fluid Mechanics*, Environmental Science and Engineering, DOI: 10.1007/978-3-319-00116-6_23,
© Springer International Publishing Switzerland 2014

the reservoir crude oil. Of all these processes, steam injection is the most reliable, and has enjoyed by far the most commercial success. In 1988, 72 % of the total enhanced oil recovery in the U.S.A. was due to steam injection (Castanier and Gadelle 1991). Steam injection technology was the leading thermal method in the former U.S.S.R. and it represented the basement for modeling thermal recovery processes for heavy oil (Jabbour et al. 1996).

This chapter aims to describe some experiments on the method of steam flooding. Recovery by steam flooding is commonly used in heavy-oil reservoirs containing oil whose high viscosity is a limiting factor for achieving commercial oil-producing rates. It has also been considered, however, as a method for recovering additional light oil.

High-temperature steam is continuously injected into a reservoir. As the steam loses heat, it condenses into hot water which, coupled with the continuous supply of steam behind it, provides the drive to move the oil to production wells.

As the formation heats, oil recovery is increased by:

1. The heated oil which becomes less viscous, making it easier to move through the formation towards production wells.
2. Expansion or swelling of the oil aids in releasing it from the rock.
3. Lighter fractions of oil tend to vaporize, and as they move ahead of the steam they condense and form a solvent.
4. Finally, the condensed steam cools as it moves through the reservoir and results in an ordinary water flood ahead of the heated zone.

An added bonus from the use of steam in both steam flooding and cyclic steam stimulation is the flushing of liners and casing perforations, as well as the reduction of deposits that may build up in the wells. Possible flow restrictions to oil production through the wells are thus reduced (United Energy Group, Enhanced Oil Recovery 2008).

In order to understand this phenomenon, it is very important to have an experimental previous study. Therefore, we present some experiments in tubes filled with sand with different particle diameters, simulating the steam injection in a porous media.

2 Experiments

The experiments have been carried out by controlling the variables that are involved, such as the pressure, temperature and steam flow rate, all in cylindrical pipes filled with homogeneous sand.

The first problem was the control of the pressure, temperature and flow rate. We used a high resolution digital camera (Nikon, 16 megapixels) to measure the fluid velocity within the porous medium and to measure the temperature distribution a thermal camera FLIR SC660 was used.

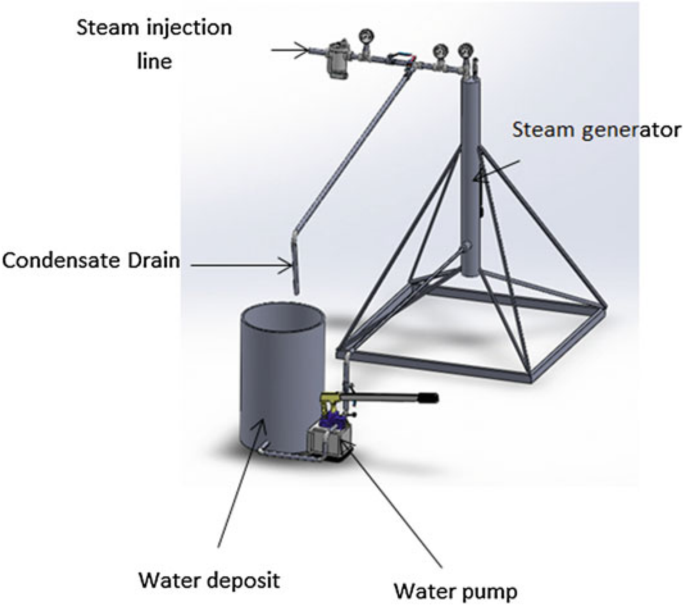

Fig. 1 Steam generator. The tube was made with an AISI 1040 steel pipe $d_t = 0.0508$ m and $L_t = 1.5$ m with a capacity of 4 lt

The steam generator was made with an AISI 1040 steel pipe with a diameter D = 0.0508 m and a length of L = 1.5 m with a capacity of 4 lt. The maximum pressure and temperature that we could reach were 8 kg/cm^2 and 120 °C respectively, see Fig. 1.

The test core is a cylindrical acrylic tube, with 0.006 m wall thickness, a length $L = 0.42$ m and a diameter $d_t = 0.039$ m, filled with a homogeneous mixture of two types of sand, see Fig. 2. The test sands are: Ottawa sand 850 µm mean diameter (d_O) and Veracruz sand with 315 µm mean diameter (d_V).

We made experiments with the material mentioned above, at different pressures $p = 0.25, 0.5$ and 1 kg/cm^2.

The first experiment was made under the following conditions: p = 0.25 kg/cm^2, $T_{initial} = 26$ °C, $T_{final} = 81.6$ °C. Volume of condensed fluid 50 ml, v = 0.03604 m/s and $Q = 0.00004305$ m^3/s, or 43.05 ml/s.

For this pressure, the gravitational force is very important in the displacement of the steam. We observe that in the bottom, the condensate forms a protuberance due to the force of gravity see Fig. 3.

For the second experiment we obtained a displacement within the matrix at a steam pressure of 0.5 kg/cm^2, an initial temperature of 26 °C and a final temperature of 83.3 °C, v =0.07157 m/s and Q = 0.00008549 m^3/s or 85.49 ml/s see Fig. 4.

In the third experiment steam injection pressure reached 1 kg/cm^2 in the porous media. Figure 5 shows the photograph of the displacement of the steam and a con-

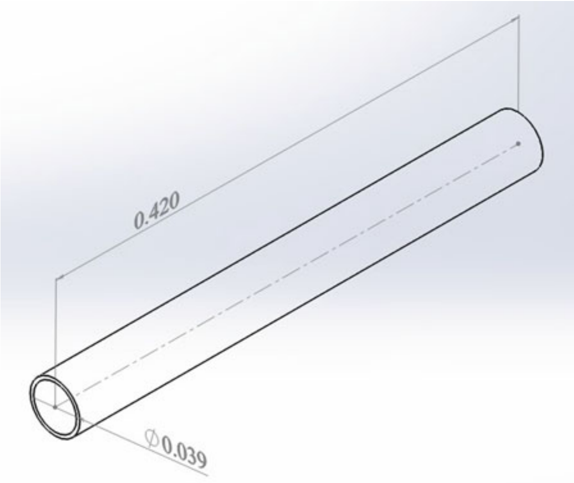

Fig. 2 Acrylic cylinder with a wall thickness of 0.06 m, $L = 0.42$ m and $\phi_{\text{test tube}} = 0.039$ m

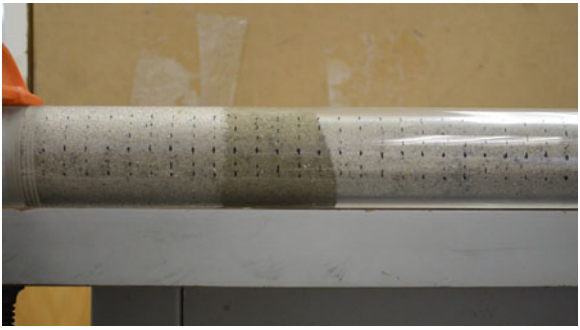

Fig. 3 Condensed profile in a homogeneous matrix formed in Ottawa sand, with an injection pressure of 0.25 kg/cm^2. As seen in the photograph, at the bottom of the specimen, bulges condensate due to the effect of the gravitational force on the experiment

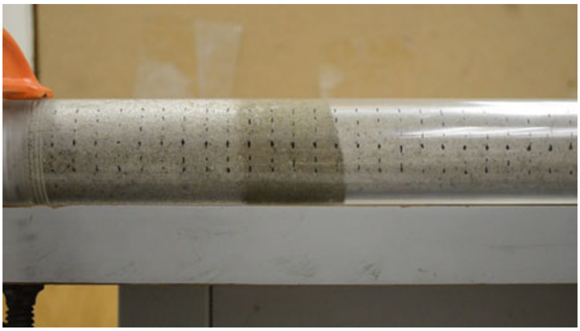

Fig. 4 Displacement with $p = 0.5$ kg/cm^2, the gravity force forms a protuberance

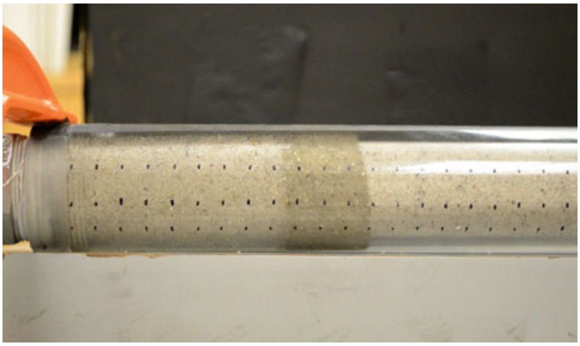

Fig. 5 Profile observed in the homogeneous matrix with steam injection at the pressure of 1 kg/cm^2

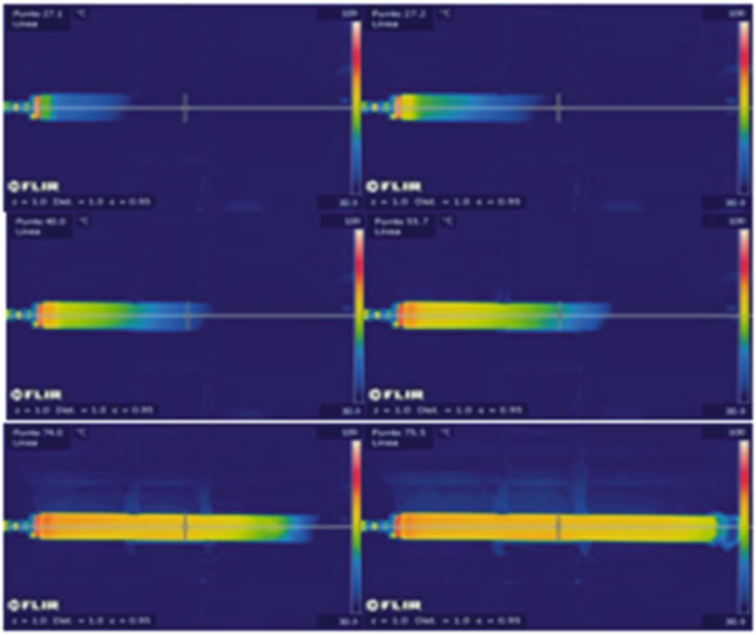

Fig. 6 Thermal sequence with steam injection at a pressure of 0.25 kg/cm^2, a homogeneous matrix consisting of sifted Veracruz sand with $d = 315$ m. The temperature is distributed evenly through the homogeneous matrix homogeneous, over time the temperature converges to 81.6 °C

densation front caused by the temperature difference in the porous media (the porous media temperature was 21 °C).

In Figs. 3, 4 and 5, we can see how the condensation front changes by the increase of the pressure and the steam flow rate. The profile shows how the flow is transformed to a type piston flow.

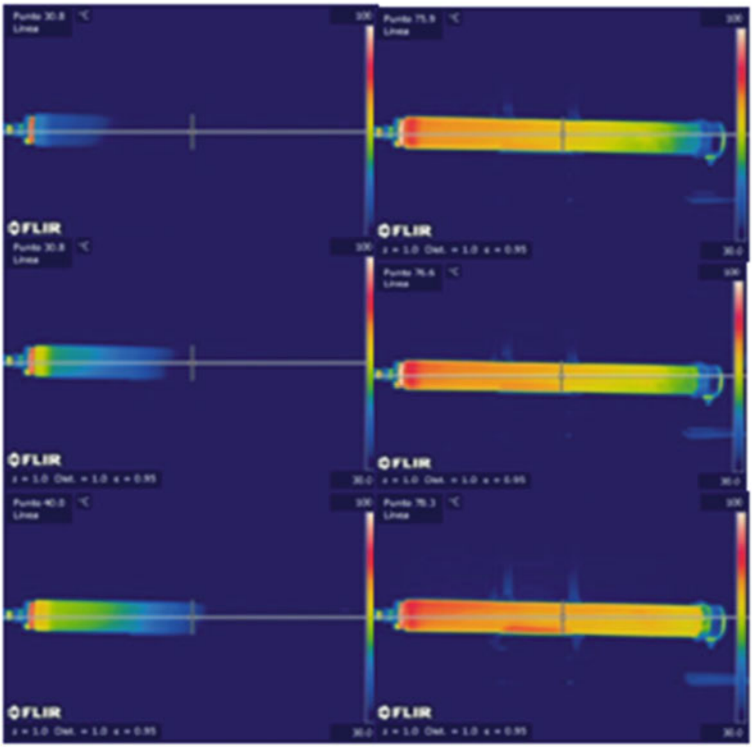

Fig. 7 Sequence of thermal photographs of the homogeneous matrix obtained with a FLIR camera, at a steam pressure of 0.5 kg/cm^2, with an initial temperature of 26 °C and a final temperature of 83.3 °C and volumetric flow of 85.49 ml/s

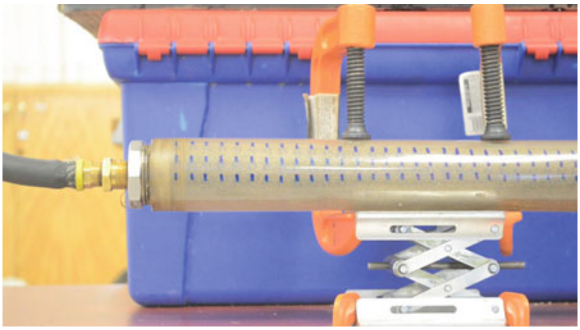

Fig. 8 Homogeneous matrix (Veracruz sand) where the thermal pictures were taken with a FLIR SC-660 camera each 10 s during all the experiment

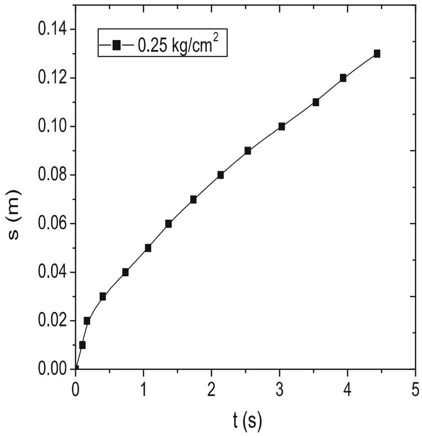

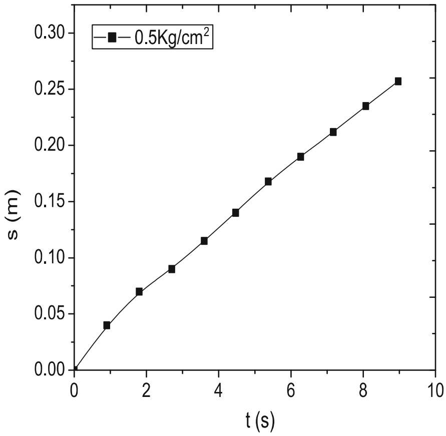

Fig. 9 Graphs of the steam displacement in the porous medium with Veracruz sand at $p = 0.25\,\text{kg/cm}^2$ and $p = 0.5\,\text{kg/cm}^2$

To observe the change of temperature, we have recorded the temperature gradient along the test tube in two different cases, with a thermal camera, as it can be seen in Fig. 6 for the case $0.25\,\text{kg/cm}^2$.

Figure 7 shows the sequence of the temperature distribution in the homogeneous porous matrix. The temperature distribution profiles are different because of the different pressures. In Fig. 6 $p = 0.25\,\text{kg/cm}^2$, and in Fig. 7 the pressure is $p = 0.5\,\text{kg/cm}^2$.

In the thermal pictures the homogeneous matrix is formed with Veracruz sand in both cases (see Fig. 8). This could be done because the low permeability of the sand from Veracruz allows a better reading of the thermal camera, and therefore shows profiles with better approximation.

3 Results

The graphs show the progress of the steam as a function of time. At the beginning, the steam shows a higher velocity. After a few seconds it slows down until it reaches the end of the test core. The final speed increases with increasing pressure (see Fig. 9).

For the case of the increase of temperature for $p = 0.25\,\text{kg/cm}^2$ and $p = 0.5\,\text{kg/cm}^2$, the maximum temperatures are 81.6 and 83.3 °C measured with a FLIR camera (Fig. 10), there is a difference of temperatures between the real measurement and the measured with the camera due to the acrylic cover, we know this difference is of 12 °C.

Figure 11 shows the displacement of the steam in the porous medium at a pressure of $1\,\text{kg/cm}^2$. Notice that the graph is a straight line.

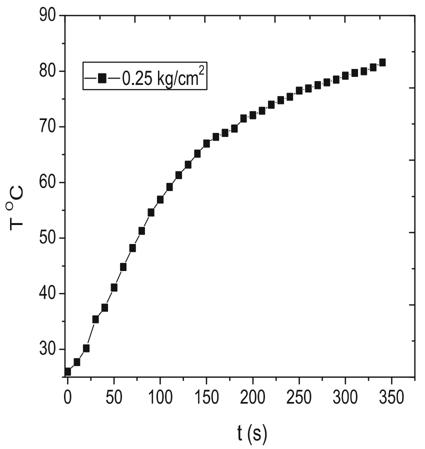

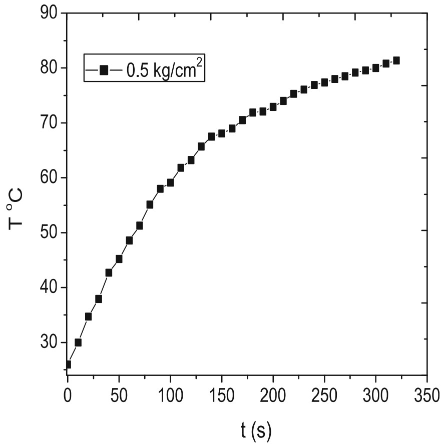

Fig. 10 Graphs of the increase of the temperature with time for Veracruz sand at $p = 0.25\,\mathrm{kg/cm^2}$ and $p = 0.5\,\mathrm{kg/cm^2}$

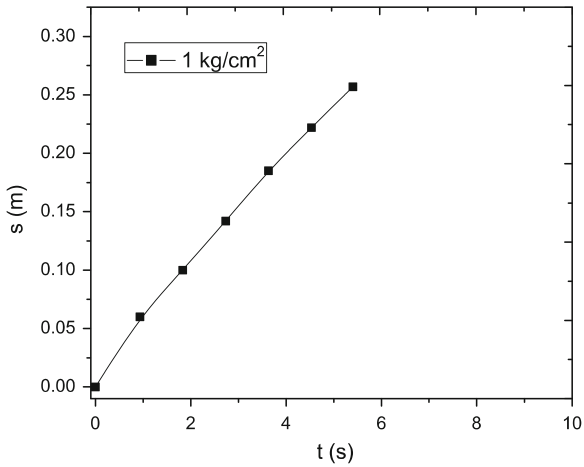

Fig. 11 Graph of the steam displacement in the porous medium with Ottawa sand for $p = 1\,\mathrm{kg/cm^2}$

Comparing 0.5 and $1\,\mathrm{kg/cm^2}$, see Fig. 12, the slope changes due to the pressure and the velocity inside the porous media. With the pressure of 0.25, see Fig. 10, we can see that the gravity force domain and the displacement is not proportional.

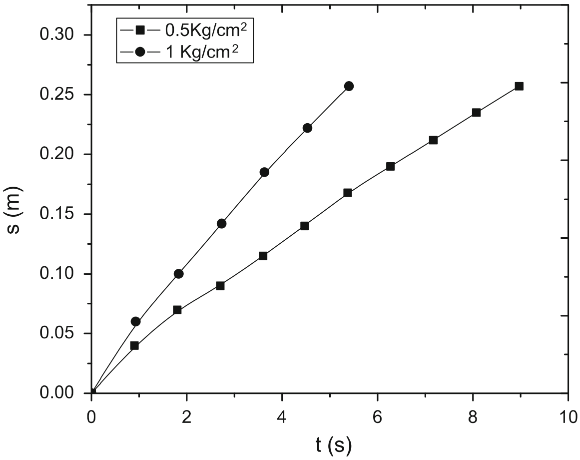

Fig. 12 comparison of the experiment with different steam pressures $p = 0.5\,\text{kg/cm}^2$ and $p = 1\,\text{kg/cm}^2$

4 Conclusions

In this work we have shown the basic experiments in which is involved the easiest arrangement (porous media and steam). This is the first step to understand their behavior into several conditions, for example at different pressures. The next step is to complicate the situation introducing a new fluid such as light and heavy oil for understanding how these fluids are going to behave during steam injection. The experiments show the real behavior of the steam in the porous media.

Acknowledgments SP and AT wish to thank the IMP and CONACYT for their fellowships. AM and AL wish to thank IMP-CONACYT-IPN for the support to the project "Análisis de mecanismos en procesos de recuperación mejorada por inyección de fluidos calientes y agentes espumantes con propiedades modificadoras de la mojabilidad". Finally, AM also thanks the IMP for his sabbatical.

Appendix

Properties of steam

Below we have the following characteristics of the steam.
Properties of steam at 0.25 kg/cm^2:

Pressure		0.25	kg/cm^2
Saturation temperature		106.188	°C
Specific entalphia of water	(h_f)	445.24	kJ/kg
Specific entalphia of evaporation	(h_{fg})	2240.21	kj/kg
Specific entalphia of steam	(h_g)	2685.45	kj/kg
Density of steam		0.731769	kg/m^3
Specific volume of steam	(V_g)	1.36655	kg/m^3
Specific entropy of water	(s_f)	1.37636	kj/kg K
Specific entrophy of evaporation	(s_{fg})	5.90557	kj/kg K
Specific entrophy of steam	(s_g)	7.28193	kj/kg K
Specific heat of steam	(c_v)	1.54032	kj/kg K
Specific heat of steam	(c_p)	2.06686	kj/kg K
Speed of sound		475.913	m/s
Dinamic viscosity of steam		1.25E$_{05}$	Pa s
Isentropic coefficient	(k)	1.31656	
Comppressibility factor of steam		0.982271	

Properties of steam at 0.5 kg/cm^2:

Pressure		0.5	kg/cm^2
Saturation temperature		111.45	°C
Specific entalphia of water	(h_f)	467.45	kj/kg
Specific entalphia of evaporation	(h_{fg})	2226	kj/kg
Specific entalphia of steam	(h_g)	2693.51	kj/kg
Density of steam		0.864345	kg/m^3
Specific volume of steam	(V_g)	1.15695	kg/m^3
Specific entropy of water	(s_f)	1.4346	kj/kg K
Specific entrophy of evaporation	(s_{fg})	5.78782	kj/kg K
Specific entrophy of steam	(s_g)	7.22243	kj/kg K
Specific heat of steam	(c_v)	1.55322	kj/kg K
Specific heat of steam	(c_p)	2.08789	kj/kg K
Speed of sound		478.49	m/s
Dinamic viscosity of steam		1.27E$_{05}$	Pa s

Properties of water at 1 kg/cm^2

Pressure		1	kg/cm^2
Saturation temperature		120.44	°C
Specific entalphia of water	(h_f)	504.426	kj/kg
Specific entalphia of evaporation	(h_{fg})	2202.01	kj/kg
Specific entalphia of steam	(h_g)	2706.44	kj/kg
Density of steam		1.12564	kg/m^3
Specific volume of steam	(V_g)	0.888386	kg/m^3
Specific entropy of water	(s_f)	1.52938	kj/kg K
Specific entrophy of evaporation	(s_{fg})	5.59889	kj/kg K
Specific entrophy of steam	(s_g)	7.12827	kj/kg K
Specific heat of steam	(c_v)	1.57627	kj/kg K
Specific heat of steam	(c_p)	2.12621	kj/kg K
Speed of sound		482.559	m/s
Dinamic viscosity of steam		1.30E$_{05}$	Pa s
Isentropic coefficient	(k)	1.3138	
Comppressibility factor of steam		0.975884	

References

Castanier LM, Gadelle C (1991) Hot fluid injection: basic concepts in enhanced oil recovery processes. In: Bavitre M (ed) Elsevier applied science. Crit Rep Appl Chem 33:271–312

Jabbour C, Quintard M, Bertin H, Robin M (1996) Oil recovery by steam injection: three-phase flow effects. J Petrol Sci Eng 16:109–130

United Energy Group, Enhanced Oil Recovery (2008) U.S. Department of Energy, National Energy Technology Laboratory

Chung KH, Butler RM (1989b) A theoretical and experimental study of steam-assisted gravity drainage process. In: Meyers RF, Wiggings EJ (eds) The fourth UNITAR/UNDP international conference on heavy crude and tar sands, vol 4. In-Situ recovery, AOSTRA, Edmonton, pp 191–210

Woods AW, Fitzgerald SD (1993) The vaporization of a liquid front moving through a hot porous rock. J Fluid Mech 251:563–579